[redacted]

ROCKETDYNE

A [illegible] VIATION, INC.

[illegible] $ _____

OFST[illegible] PRICE(S) $ _____

Hard copy (HC) 2.00

Microfiche (MF) .50

ff 653 July 65

N67 12914
(ACCESSION NUMBER) (THRU)

44 1
(PAGES) (CODE)

CR 80156 12
(NASA CR OR TMX OR AD NUMBER) (CATEGORY)

FACILITY FORM 602

ROCKETDYNE
A DIVISION OF NORTH AMERICAN AVIATION, INC.
6633 CANOGA AVENUE, CANOGA PARK, CALIFORNIA

R-6693-1

SUMMARY, STUDY OF PUMP DISCHARGE PRESSURE OSCILLATIONS

Contract NAS8-20143
G.O. 8739

PREPARED BY

E. D. Jackson

APPROVED BY

K. Rothe
Chief
Turbomachinery Specialties

NO. OF PAGES 27 & vii

REVISIONS

DATE October 1966

DATE	REV. BY	PAGES AFFECTED	REMARKS

FOREWORD

This report is a summary of the work conducted under G.O. 8739 in compliance with Contract NAS8-20143.

ABSTRACT

An analytical investigation was conducted of pump-generated pressure and flow oscillations, and analytical procedures were developed which may be applied to the design and analysis of turbopumps from an oscillation standpoint. The pump blade wake oscillations were studied from the viewpoint of the generation of oscillation waves; the transmission of waves in the pump discharge system; the reinforcement, or superposition, of waves in the pump discharge from multiple sources; and the elimination of waves by acoustic dampers. Initial studies were made of cavitation oscillations by studying the cavity volume of an inducer and its effect on the oscillations. Experimental programs were conducted to verify and supplement certain of the analytical results. A limited experimental study was also made of stall oscillations in an axial and centrifugal pump.

CONTENTS

ILLUSTRATIONS

INTRODUCTION

Pressure and flow oscillations in the discharge system of turbopumps are a commonly observed phenomena. In most low-pressure pumps, the oscillation amplitudes are small and are not detrimental to the main function of the pumps. In high-pressure pumps, these oscillations, though still a small fraction of the total head, become significant in amplitude. The observed oscillation frequencies vary over a large range from less than 10 to 1000 or more cps. The higher frequency oscillations may cause thrust chamber stability problems or may excite vibration in structural parts of the pump and feed system. The low-frequency oscillations are limit-cycle oscillations transmitted through the feed system and result in engine thrust oscillations. These limit-cycle oscillations may couple with vehicle fluid and structural dynamics in such a way as to cause vehicle or mission failure.

Sufficient familiarity with pump-generated oscillations has been obtained at Rocketdyne to classify certain distinct types of oscillations according to their source. It is convenient to distinguish three distinct classes of oscillations which are sufficiently independent to permit an independent study of each:

1. Blade Wake Oscillations. A blade wake consists of low-energy fluid in the blade surface boundary layer. The blade wakes, combined with the main flow between wakes, form a periodic flow pattern in the blade-to-blade direction around the pump periphery. To a downstream blade row rotating relative to that upstream, the wakes of the preceding blade row appear as an unsteady flow field. This flow field is responsible for setting up acoustic

waves in the system which are measured far downstream of the blade row and which lead to resonant conditions in the system resulting in oscillation amplitudes several times larger than at off-resonance.

2. Cavitation-Induced Oscillations. The notation "cavitation-induced" oscillations refers to the low-frequency oscillations (0 to 50 cps) commonly found at the inducer inlet and in the pump discharge as the NPSH is lowered.

3. Stall Oscillations. As the flowrate through a pump is reduced from its design value, the pump head is increased by virtue of the increased blade loading. At some value of the flow, the blade loading will reach a limit, the blades will stall, and, generally, some form of unsteady flow will result.

Essentially, all aspects of the blade wake oscillations were considered, i.e., the oscillation generation, transmission, reinforcement or superposition, and damping. The cavitation and stall oscillation analyses were not as extensive as those of the blade wake oscillations. The program is primarily analytical, the experimental phases being designed to corroborate and supplement the analytical results.

BLADE WAKE OSCILLATIONS--GENERATION OF ACOUSTIC WAVES

The velocity leaving a blade row is nonuniform due to both the gradients in the region designated as the potential flow and the viscous boundary layers along the blade surfaces, but is periodic in the mean, the period extending from blade to blade. This nonuniform velocity would appear to a downstream blade row in relative motion to the upstream blade row as a periodic unsteady velocity field which produces unsteady pressures on the downstream blades. Both the unsteady velocity field at the entrance of the blade row and the unsteady pressures are responsible for the generation of acoustic pressure waves. Therefore, a complete analysis of the generation of blade wake oscillations would involve the following tasks:

1. Compute the nonuniform velocity field at the exit of the upstream blade row by performing a:
   a. Potential flow analysis
   b. Boundary-layer analysis
2. Given an unsteady velocity field (which would be the nonuniform field calculated in 1 above or measured experimentally), calculate:
   a. The acoustic waves generated by the unsteady velocity at the entrance of the blade row
   b. The unsteady blade pressure loads due to the unsteady velocity field
   c. The acoustic waves generated by these unsteady pressure loads

Task 1 above is secondary to the main objective of the current study and was not pursued to any large extent. A stream filament method for calculating the flow in the blade-to-blade plane of a centrifugal pump was

developed and yielded good results for an example radial impeller problem. A survey was also made of the literature to determine a method of estimating the boundary layer in a turbopump rotor, but no adequate method was available due to the complexity of the problem.

A primary effort was made to indicate the relative importance of the acoustic waves generated by the two related mechanisms indicated in Tasks 2a and 2c. Before this could be done, Task 2b had to be performed to indicate the amplitude of the unsteady pressures on the downstream blade row. In the literature, these unsteady pressures have been investigated as a function of four effects which have been designated as the circulation, blade thickness, wake, and wake distortion effects. The analytical development of each is based primarily on the two-dimensional theory of the unsteady flow about a thin airfoil. Only the viscous wake effect was adopted for use in the current program, a computer program being written to calculate the unsteady pressures on a blade due to an approaching arbitrary wake velocity.

The generation of waves into a medium surrounding a plate by unsteady forces on the plate surface is a coupled problem requiring solution of the equation of motion for transverse displacement of the plate as well as solution of the wave equation in the medium. The two solutions are coupled by the boundary conditions which require continuity of both the normal velocity and pressure across the fluid-plate interface. To estimate the order of magnitude of the wave amplitude generated by this coupled motion, a simpler example problem discussed in Ref. 1 was considered. This example problem consisted of a plate of infinite extent and uniform thickness. The fluid medium above the plate was assumed to be coupled to the plate motion, but the fluid below the plate was not. The coupled equations were solved, yielding for this example problem an expression for the amplitude of the waves generated by an unsteady force on the plate.

To estimate the order of magnitude of the amplitude of the waves generated by an unsteady velocity boundary condition at the inlet of a blade row (or duct), a second simple example was assumed. This example consisted of a straight, infinite, rectangular duct with a simple harmonic velocity at its inlet boundary, which velocity was uniform in the plane of the duct. The wave equation was solved to yield the generated wave amplitude.

Typical Mark 10 pump data were then used to compare the amplitudes of the waves generated by these two sources. This comparison indicated that the amplitude of the waves generated by the pressure loadings, corresponding to Task 2c above, were less by a factor of 10^4 to 10^5 than those generated by the velocity boundary condition. Thus, the tasks denoted as 2b and 2c need not be considered in calculating the pump blade wake oscillation amplitudes.

A test program was conducted in support of the analytical investigation. The primary objective was to establish experimentally typical velocity fields at the discharge of centrifugal impellers as a function of distance from the impeller. Secondary objectives included measuring the dynamic pressures on a volute tongue and measuring the dynamic pressures downstream due to the acoustic waves to attempt a correlation with the velocity field data. The tests were conducted in the Mark 10 air rig using two each LOX and fuel pumps with impellers of both 6 full vanes and 6 full/6 splitter vanes. The velocity data were obtained with two hot-wire anemometer modules, but the data from one of the modules was later found to be consistently yielding velocities which were too low.

Some typical data obtained from the Mark 10 6+6 impeller fuel pump are shown in Fig. 1. The velocity vector shown is the vector sum of the radial and tangential unsteady components which, except for secondary flows,

Total Velocity Vector As A Function Of Radial Distance (R)
From The Impeller Tip

6+6 Vane Impeller - Air Rig Facility
Speed = 2100 rpm - Nominal Flow

STATION A-1

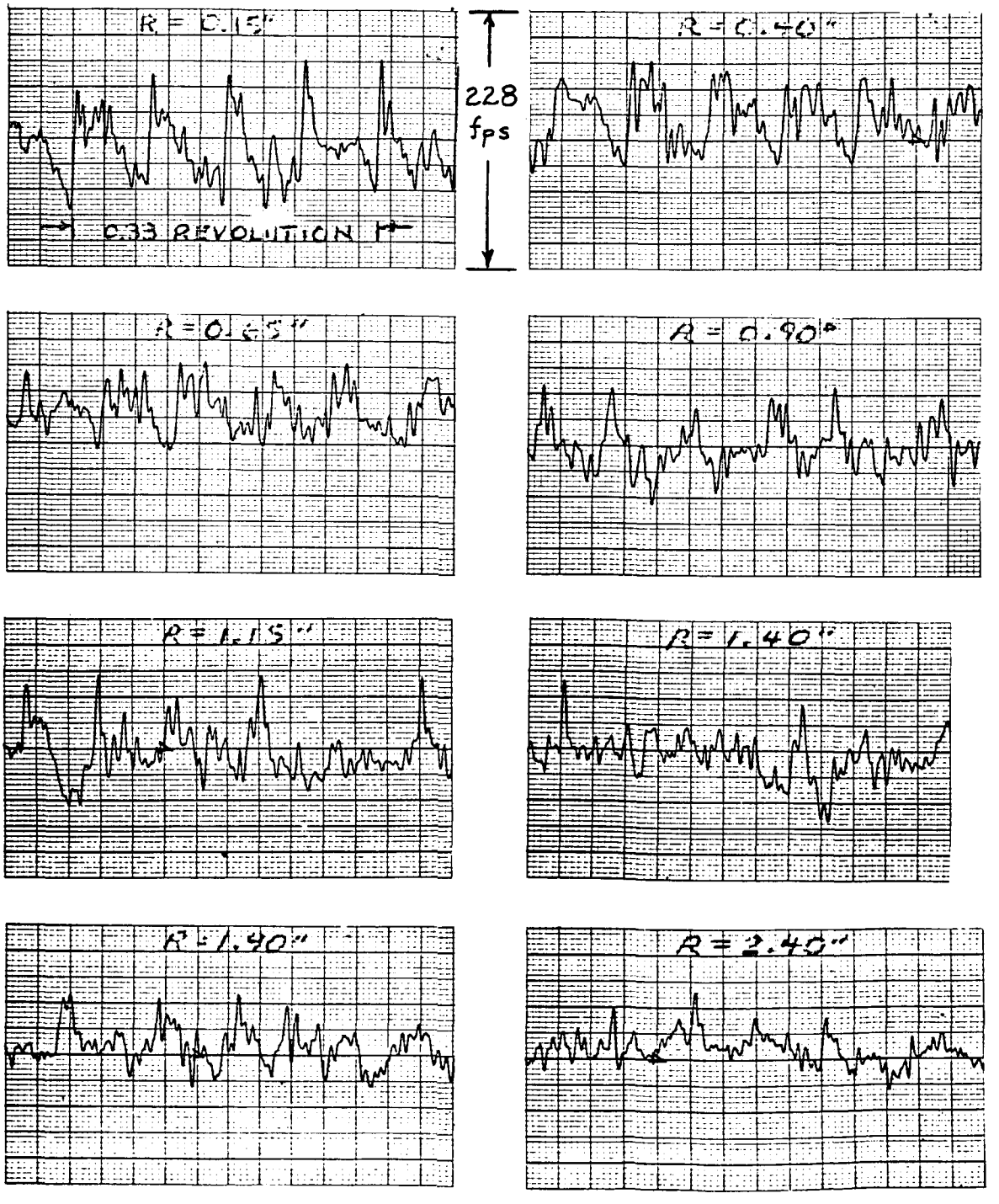

Figure 1. Velocity Oscillations at the Mark 10 Fuel Impeller Discharge

represents the total velocity vector. The wave shape near the impeller, the clarity of the data, and the relative amplitude as a function of distance from the impeller, are of interest. Data of this type were analyzed to determine an average amplitude of the unsteady velocity at a distance of approximately 0.125 inch from the impeller tip. The ratio of this average unsteady velocity amplitude to the difference in the impeller tip speed and the mean fluid velocity in the volute was found to be approximately 1.0, indicating lower oscillation amplitudes for a high-head pump operating at a fixed speed.

Data from five successive pump revolutions were manually superimposed to indicate the average blade wake velocity profile and the extent of the variations from this average near the impeller tip. The total velocity vector at a distance of 0.125 inch from the impeller indicated a strong time correlation. The radial component did not indicate as much correlation.

A typical plot of the relative velocity vs the radial distance from the impeller is shown in Fig. 2. This relative velocity is defined on the figure, and indicates the rate of mixing and subsequent smoothing of the velocity variations. The average amplitudes of the unsteady pressures on the leading edge of the volute tongues were also determined. These values ranged from 0.01 to 0.038 psi. Using data from one of the pumps, this pressure was computed using the viscous wake effect theory and found to be 0.023 psi, in good agreement with the data.

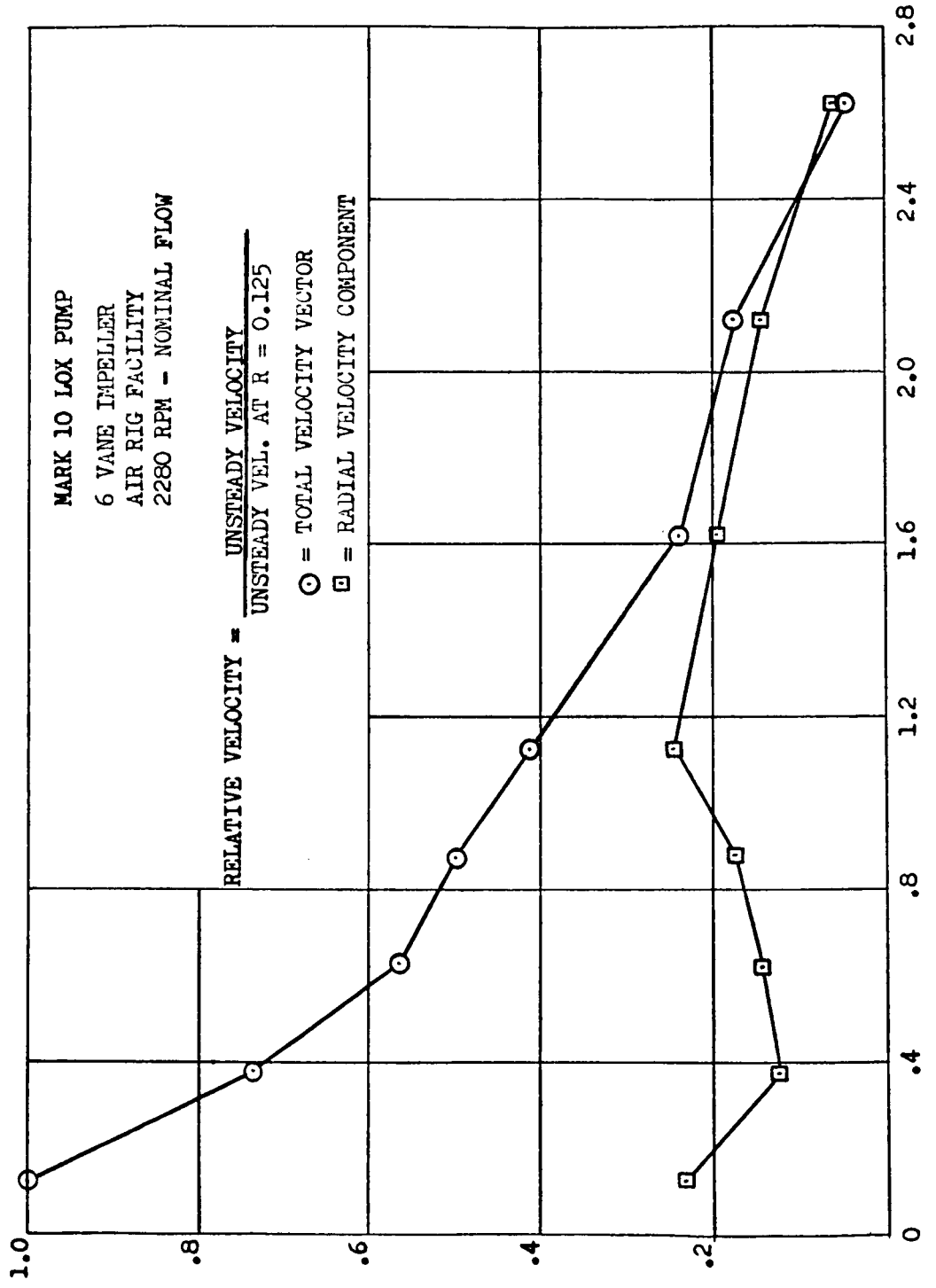

Figure 2. Relative Unsteady Velocity Amplitude vs Distance From Impeller Discharge

BLADE WAKE OSCILLATIONS--TRANSMISSION OF ACOUSTIC WAVES

The effective amplitudes of the blade wake oscillations of the turbopump are strongly dependent on the system through which the oscillations are transmitted. The acoustic properties of this system must be adequately defined before either calculation of the estimated amplitudes or explanation of experimental amplitudes can be made. The primary objective of this phase of the current study was to investigate the acoustic properties of certain elements commonly found in engine or test facility pump systems.

The general theory of the transmission of waves in a source-free, non-viscous medium in a straight duct was reviewed. The solution of the wave equation was given in terms of the eigenfunctions and eigenvalues capable of describing a general wave. This solution was then reduced to the plane wave case, and reflected waves were added to yield the familiar "time-delay" equations which were used extensively in the analysis of the data. The transmission of waves in discontinuities was then considered where a discontinuity is any element which causes a deviation from a uniform straight duct. The discontinuities considered in the present study were elbows, valves, orifices, and volutes.

If it is assumed that the compressibility of the fluid can be neglected within the bounds of the discontinuity, the flow within these bounds obeys the Laplacian equation rather than the wave equation. If the discontinuity is also assumed to be symmetric so that the velocity and velocity potential are identical at its entrance and exit, then the discontinuity can be treated as a plane transformer, i.e., plane discontinuity, connecting two arms of an infinite pipe. The transformer requires continuity across its boundary of both the velocity potential and the velocity. This technique is presented in Ref. 2.

Both mitered and curved elbows were studied by this technique of plane discontinuities. The solution was obtained for the apparent inertance of the elbows in the form:

$$L = 2G \rho \ell_x / S \text{ for mitered elbows} \quad (1)$$

and

$$L = 2G \rho (R_1 - R_2)/S \text{ for curved elbows} \quad (2)$$

where ρ is the fluid density, ℓ_x the width of a two-dimensional channel, R_1 and R_2 the outer and inner elbow radii, respectively, and S is the duct cross-sectional area. The values obtained for the constant 2G for different elbow turning angles φ were:

φ \ R_2/R_1	0.50	0.20	0.10	0.01	Mitered
30 degrees	0.088	0.16	0.18	0.20	0.22
60 degrees	0.10	0.22	0.28	0.37	0.41
90 degrees	0.10	0.24	0.34	0.50	0.58

The total elbow impedance consists of the inertance value determined by either Eq. 1 or 2 plus the inertance, compliance, and resistance of the elbow treated as a straight pipe with length equal to the centerline length of the elbow. This resistance must be determined from experimental data for the energy lost in flowing through the elbow.

The valves were assumed to be representable by a plane barrier located in an otherwise uniform two-dimensional duct. This barrier also represents a plane discontinuity. The case of the barrier located symmetrically in the duct was analyzed for several ratios of blocked area. The

inertance computed was of the same form as given in Eq. 1. Letting a/ℓ_x equal the unblocked to total area ratio, the following values of the constant 2G were obtained:

a/ℓ_x =	0.05	0.10	0.20	0.30	0.40	0.50	0.75
2G =	3.23	2.37	1.50	1.05	0.67	0.44	0.097

For a poppet valve sitting in an elbow, as occurs in the Mark 10 pump discharge lines, this inertance would have to be added to the total impedance of the elbow portion. If the valve does not restrict the flow by decreasing the cross-sectional area, then it would be represented by a barrier with zero width and, thus, with zero inertance.

The impedance of orifices has been the subject of previous investigations which are reported in the literature. The orifice resistance consists of a radiation term, a viscosity term with a correction for heat conductivity, and a velocity term. The reactance term is formed from the classical mass expression with a correction for both velocity and wall interaction effects.

The distinguishing characteristic of a volute is that its cross-sectional area is changing as a function of the distance traveled along the volute axis. Thus, the volute was treated as a horn with a linear area-to-distance relationship which is characteristic of most volutes. Plane waves were assumed so that the wave equation with the linear area-to-distance characteristic reduces to a modification of Bessel's equation which can be readily solved in terms of Bessel functions. However, although the volute horn equation is readily solved, the solution is not in a form convenient for use in any system frequency-response analysis. Therefore, the impedance of the volute must be approximated by dividing the volute into a number of segments, each representing a step change in cross-sectional area. Using an average area for each segment, its resistance, inertance, and compliance can be computed in the same manner as for a segment of straight pipe.

An experimental program was conducted to verify and supplement the analytical results. The tests were conducted in air using a horn driver actuated by an oscillator through a power amplifier as the acoustic wave source. Tests were conducted in simple systems consisting of straight pipes with an included elbow, valve, tee joint, conical horn, or orifice. The frequency was ramped from 50 to 4000 cps in each test, but only the data in the lower-frequency range were analyzed.

The objective of the analysis of the data was to express the impedance of each element tested in proper parametric form and to solve for the parameter values to compare these with their predicted values. Suitable analog models were developed, and a multiparameter optimization technique used to determine the unknown parameters. The optimum parameter values were reached when some defined error criterion was minimized by the optimization scheme using the test data as inputs.

The inertance of the elbows obtained from the experimental data was in fair agreement with the predicted value; however, the analytical inertance is primarily a line inertance, the portion due to the plane discontinuity calculation being a small percentage of the total. The ratio of the experimental to analytical elbow inertance was in the range 0.86 to 1.08 with an average of 0.96. The valves tested were Mark 10 valves in the wide open position such that no area reduction is obtained. In this case, the valve is assumed to act like a section of elbow, and the calculated and experimental effective inertance of the valve were in good agreement.

The orifice data did not agree with predicted values, the differences being so large that the data were suspect of being bad data. The conical horn was treated as a section of straight pipe with the same diameter as the horn discharge, and the equivalent optimum length of the straight section was approximately 28 percent of the actual horn length.

BLADE WAKE OSCILLATIONS--REINFORCEMENT OF PRESSURE WAVES IN PUMPS WITH VANED DIFFUSERS

In a pump with a multivaned diffuser, each time a rotor vane rotates past any of the diffuser vanes, acoustic waves are generated. If this multivaned diffuser feeds a scroll (or volute) with a single discharge and/or inlet, then the waves from each diffuser vane will be traveling toward a common point. If these waves reach this point at the same time, they will be superimposed, and a linear superposition was assumed. Clearly, each wave has the same frequency and similar amplitudes; however, the phase of each wave depends on its time of generation and the distance from the point of superposition to the point of origin of the wave. If each wave is exactly in phase, wave reinforcement is said to occur, and the resulting wave amplitude will be the sum of the amplitude of each of the individual waves. Similarly, the phase shift of the waves could be such as to superimpose vectorially with a zero resultant amplitude. Strub (Ref. 3) has derived an analytical solution for calculating the pump operating conditions at which wave reinforcement occurs.

Using the variables defined in Appendix A and with $Z_i > Z_d$, Strub shows that the jth harmonic of the oscillations will reinforce through phase coincidence when m is any integer such that:

$$\frac{Z_i}{Z_d}\left(\frac{Z_d - Z_i}{Z_i} + \frac{\pi D_v n}{c + v}\right) = \frac{m}{j} \tag{3}$$

Substituting

$$v = K' n/S \tag{4}$$

where K' is a constant and S is the volute discharge cross-sectional area, and solving for pump speed yields:

$$n = \frac{\left(1 - \frac{Z_d}{Z_i} + \frac{Z_d}{Z_i}\frac{m}{j}\right) c}{\left[\pi D_v - \left(1 - \frac{Z_d}{Z_i} + \frac{Z_d}{Z_i}\frac{m}{j}\right)\frac{K'}{S}\right]} \tag{5}$$

This equation permits computation of the speeds at which the jth harmonic will result in wave reinforcement.

Strub's equation assumes that the wavelength of the oscillations is large compared to the change in the mean volute diameter with distance along the volute flowpath. If this assumption is not true, as was encountered in a pump tested by Rocketdyne, the details of the actual pump geometry must be considered to calculate more accurately points of wave reinforcement.

It is again assumed that the amplitude of the wave generated at each vane is equal, and it is further assumed that each wave can be expressed as a sine function. Letting Y equal the resulting amplitude of the superimposed waves divided by the amplitude of an individual wave, then:

$$Y = \sum_{i=1}^{Z_d} \sin(\omega + \eta_i) \tag{6}$$

where ω is the circular frequency of the waves and η_i denotes the relative phase of each wave. Now η_i can be expressed as:

$$\eta_i = \frac{2\pi T_i}{\lambda} - \omega \frac{s_i}{U_t} \tag{7}$$

The variables are defined in Appendix A.

For a given pump, η_i can be readily calculated for each vane, taking into consideration the variation in the mean volute diameter.

To determine the maximum value of Y with respect to time, set dY/dt = 0 (Eq. 6) and solve for t. This yields:

$$t = \frac{1}{\omega} \tan^{-1}\left[\sum_{i=1}^{Z_d} \cos \eta_i \Big/ \sum_{i=1}^{Z_d} \sin \eta_i\right] \tag{8}$$

Substitution of Eq. 8 into Eq. 6 permits calculation of the maximum superimposed wave amplitude at any speed. Similar results can be obtained for

the case where there are more diffuser vanes than impeller vanes except that the wave reinforcement occurs at the beginning of the volute.

A Mark 26 fuel pump was tested in the air rig to confirm the analytical results. This pump has 29 impeller vanes and 19 diffuser vanes. With 29 impeller vanes, the fundamental oscillation frequency is 29 N/60 (N = pump speed, rpm), which is large enough to yield wavelengths which are not large compared to the change in the mean volute diameter. Therefore, Eq. 6 was used to compute the amplitude as a function of speed. The analytical results are given in Fig. 3. The experimental results (filtered to obtain only the component of the oscillations at the frequency 29 N/60 cps) and pump speed are given in Fig. 4.

The data show increased amplitudes in the range of 6700 to 7800 rpm, which corresponds to the region where Y exceeds a value of 9.0. The peak value of both data and Y occur at approximately 7200 rpm. The data show a slight increase in amplitude at a speed of 8400 rpm and, similarly, Y shows an increase at the same speed. However, Y does not reflect the increase in amplitude observed in the data in the range of 9400 to 10,000 rpm. The above data were obtained at nominal flow. Similar results were obtained for flows at ±30 percent of nominal. Other harmonics of the oscillation were observed and behaved as expected.

$$Y = \frac{\text{AMPLITUDE OF ALL WAVES SUPERIMPOSED}}{\text{AMPLITUDE OF A SINGLE WAVE}}$$

WITH 19 DIFFUSER BLADES: $Y_{max} = 19.0$

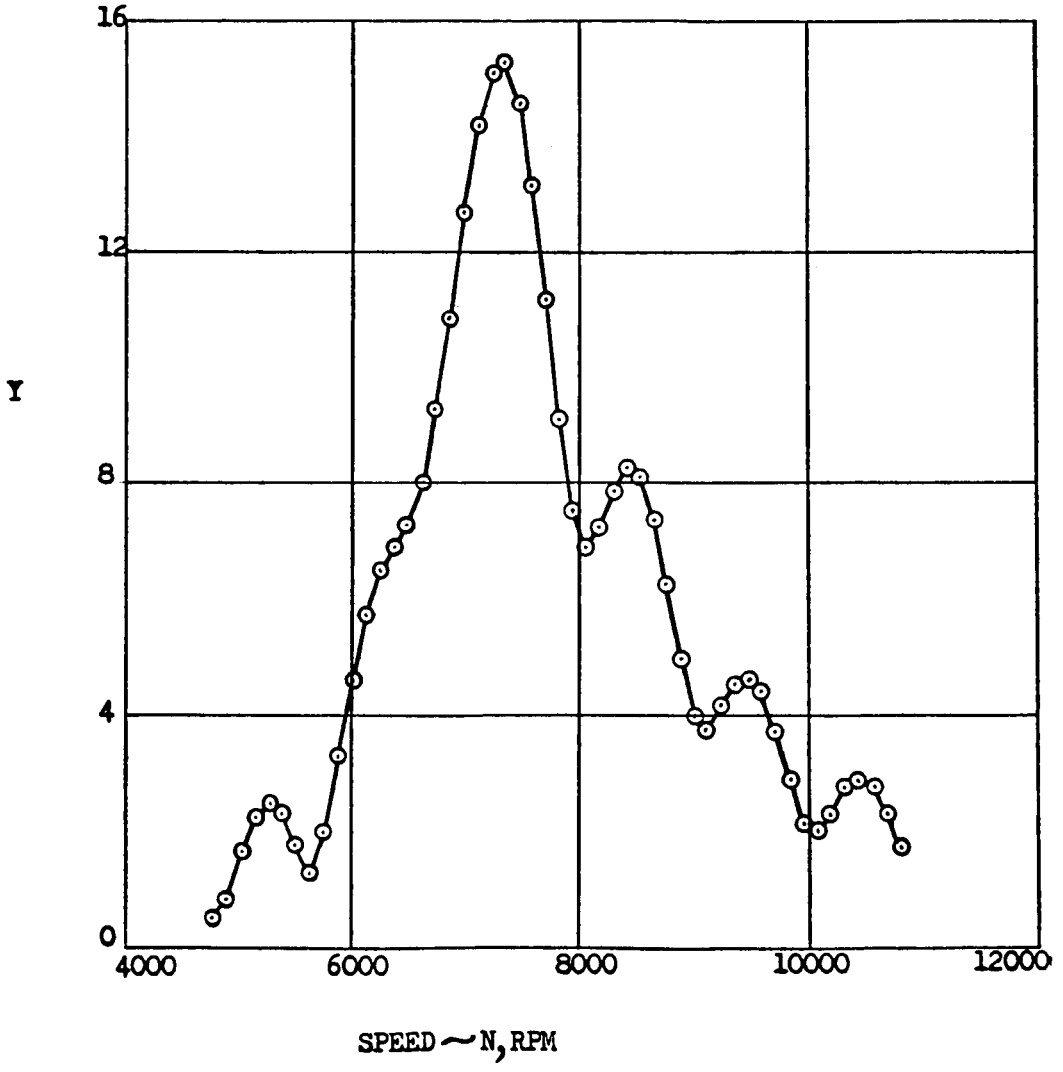

Figure 3. Relative Amplitude of Superimposed Waves in the Discharge of a Mark 26 Fuel Pump

Absolute Value of Discharge Pressure Oscillations
Filtered At Frequency = 29N

N = Pump Speed -- Flow Coefficient = 0.09375

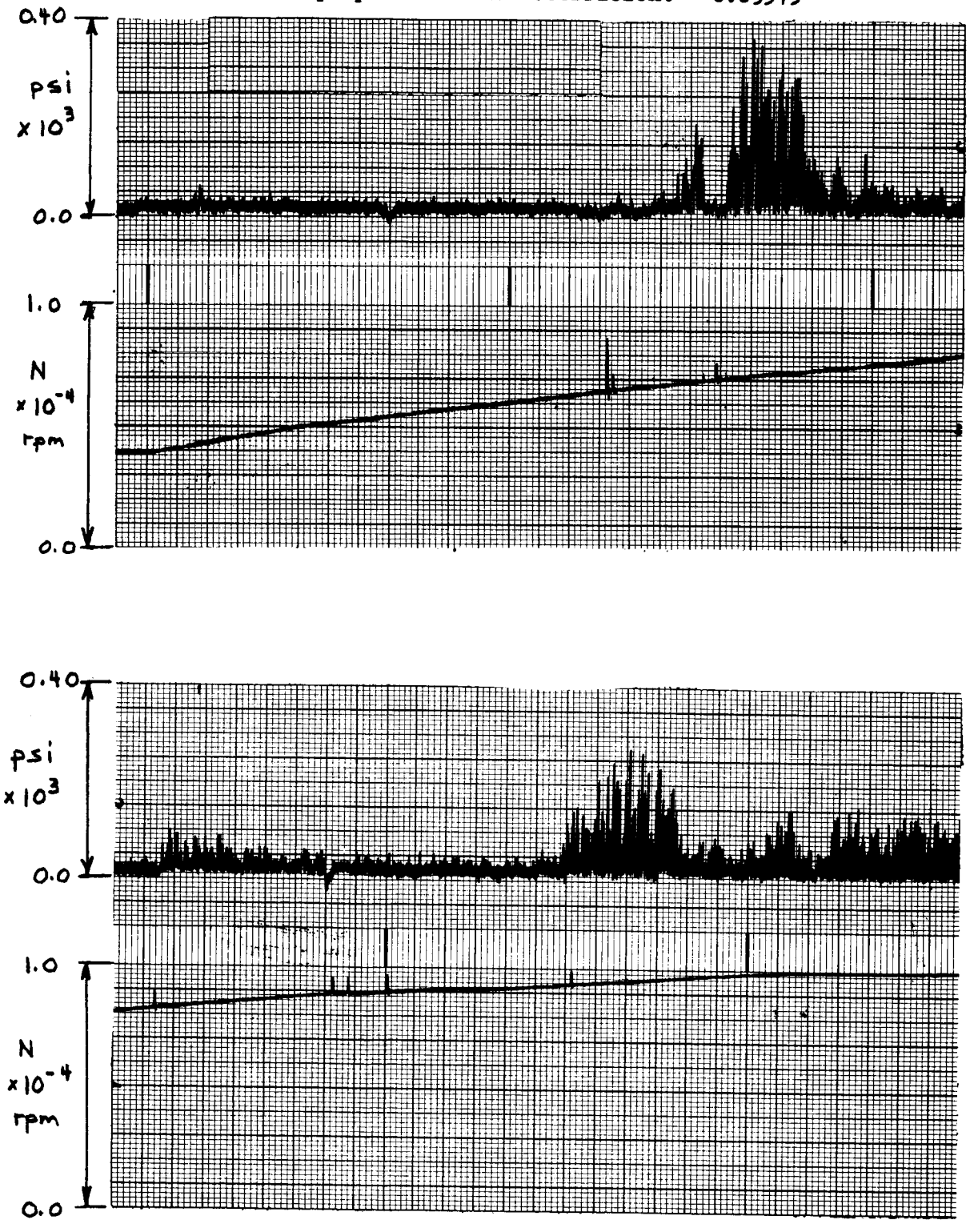

Figure 4. Air Test Data for Wave Reinforcement in Mark 26 Fuel Pump

BLADE WAKE OSCILLATIONS--ATTENUATION OF ACOUSTIC WAVES BY ACOUSTIC DAMPERS

Acoustic dampers are in general use in many fields. The intent here was simply to bring to the reader's attention the availability of these dampers and to demonstrate briefly their characteristics, and thus their feasibility for use in pump systems. Two types of dampers were considered:

1. Quarter-wave tube, capacitor, Helmholtz resonator, and Quincke tube. These dampers act effectively as a branch inertance and/or capacitance in the line.
2. Tube bundle, screens, and baffles. These act primarily as a resistance in the line.

All of these dampers are shown in Fig. 5. The theoretical filtering characteristics of all of the first type of dampers were indicated, and all of the dampers were tested using an acoustic sound source in air. The test results were analyzed on the analog computer to determine the optimum experimental parameter values defining the damper. These optimum values were then compared with the theoretical values. Results obtained for the capacitor and resonator are given below:

Damper	Parameter	Experimental Value	Theoretical Value	Units
Capacitor	Line Inertance	0.0944	0.0895	$lb\text{-}sec^2/ft^5$
	Capacitance	0.271×10^{-4}	0.271×10^{-4}	ft^5/lb
Helmholtz Resonator	Line Inertance	0.152	0.152	$lb\text{-}sec^2/ft^5$
	Capacitance	0.169×10^{-4}	0.179×10^{-4}	ft^5/lb

With only an acoustic flow, i.e., no steady flow, the resistance in all the tests was low compared to any line inertance. Therefore, the resistance values of the tube bundle, screens, and baffles could not be determined experimentally.

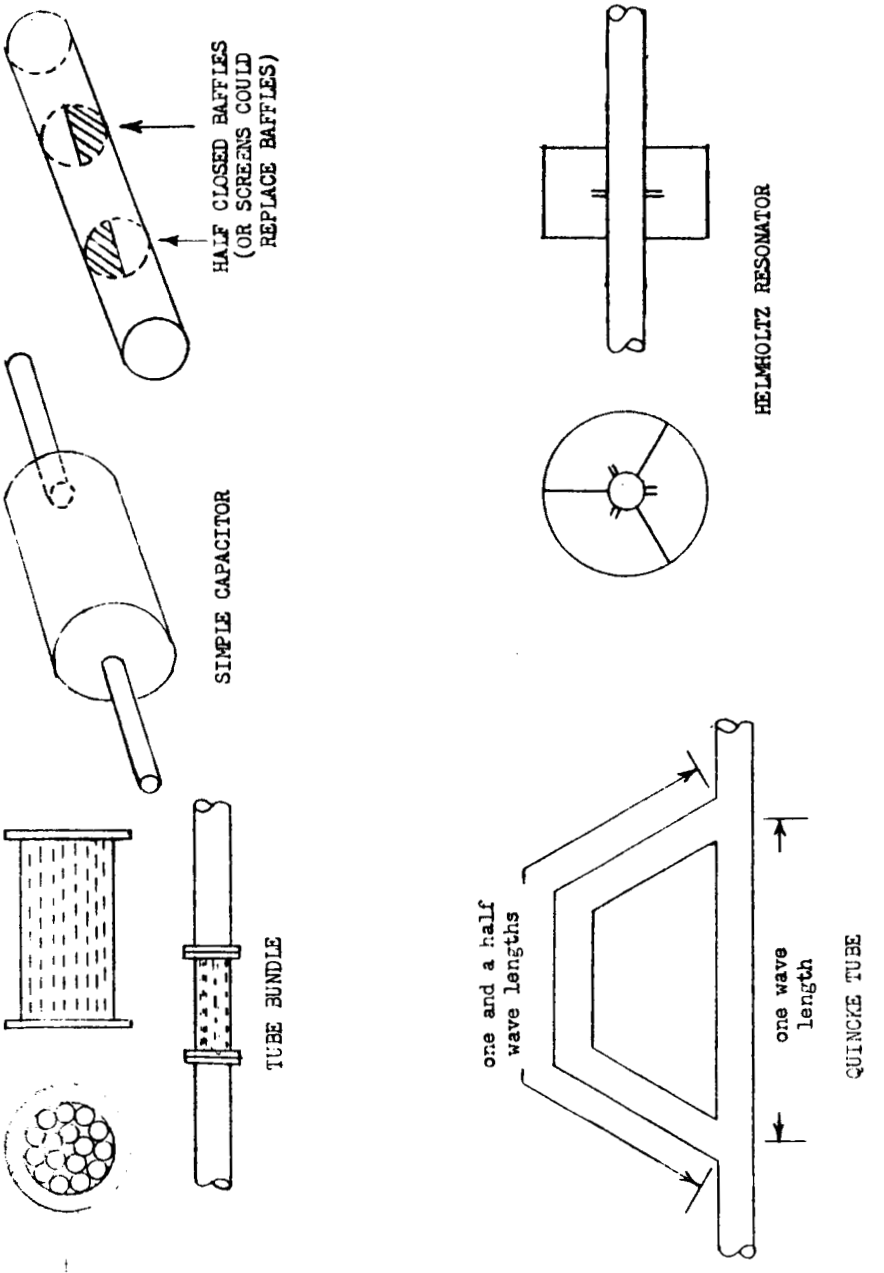

Figure 5. Acoustic Damper Concepts

CAVITATION-INDUCED OSCILLATIONS

In the process of improving pump suction performance, pump inducers have been required to operate at low values of NPSH. As a result, the flow becomes increasingly unstable due to the occurrence of partial or limited cavitation on the suction side of the inducer vanes. The present effort was concentrated on describing the mechanism of oscillations related to the formation of finite cavities at the blade leading edges as the principal mode of cavitation, thus neglecting the possible effect of a second mode of cavitation involving two-phase flow, as well as the effect of tip vortexes. In this case, the unsteady flow phenomena in the inducer can be described in terms of the continuity condition applied to the inducer inlet and discharge flow giving the cavity size as a function of the excess of discharge over inlet flow on the one hand, and in terms of the free streamline theory for a cavitating potential flow on the other hand.

The continuity condition expresses the cavity volume as:

$$V_c = (\rho g)^{-1} \int (\dot{w}_2 - \dot{w}_1)\, dt \qquad (9)$$

where $\dot{w}_2$ and $\dot{w}_1$ are discharge and inlet flowrate, respectively, and ρ is the density. The cavitating flow in the inducer is assumed to be described by the free streamline wake theory given in Ref. 4. A computer program was written to evaluate the free streamline theory to obtain the cavity area as a function of cavitation number and angle of incidence of the inducer flow. A second computer program was written to express this area by a suitable relationship (curve fit) for use on the analog computer. The cavity volume computed from these two programs was expressed in the form:

$$V_c = \frac{4}{3}\frac{\pi^2}{N_B} (r_T^3 - r_H^3)\, S_n \qquad (10)$$

where S_n is the net cavity area given by:

$$S_n = \sum_{j=o}^{2} \sum_{i=o}^{3} a_{(1+i+4j)} \alpha^j \tau^i \tag{11}$$

where α and τ are angle of incidence and cavitation parameter at the tip, respectively.

Equations 9, 10, and 11 are three of the quasi-steady equations describing the dynamics of a cavitating inducer. The other equations required are:

$$\varphi = \dot{w}_1 / \rho g S_1 U \tag{12}$$

$$\alpha = \beta - \text{Arctan } \varphi \tag{13}$$

$$\tau = \frac{P_1 - P_v}{0.5 \rho U^2} + \varphi^2 \tag{14}$$

$$(P_2 - P_1) = \rho U^2 (b_o + b_1 \varphi + b_2 \varphi^2) \psi_2 \tag{15}$$

$$\psi_2 = \begin{cases} 1.0 \text{ if } \tau \geq 0.8 \\ (b_3 + b_4 \tau + b_5 \tau^2 + b_6 \tau^3 + b_7 \tau^4) \text{ if } \tau \leq 0.8 \end{cases} \tag{16}$$

The variables are defined in Appendix A. The coefficients, b_i, in Eq. 15 and 16 are determined by a curve fit of the average shape of the head vs flow (Eq. 15) and head vs NPSH (Eq. 16) relationships for a given inducer.

A set of eight equations are thus derived for the dynamic model of a cavitating inducer, but the equations contain 10 unknowns, obviously requiring two input variables. Dynamic pressures are known just upstream and downstream of the inducer (i.e., P_1 and P_2); however, using these as input data yields no output data which can be compared to evaluate the theory. To permit comparison of the theory with test data would require both dynamic

pressure and flow data. Or, since dynamic flow data are not generally available, the inducer test facility must be modeled dynamically to establish two more relationships for the pressure and flow at the inducer extremities.

The Rocketdyne water tunnel was modeled by dividing the tunnel into a number of finite elements, consistent with junctions, area changes, and valves contained in the system. Each element was represented by a finite inertance and capacitance, the resistance being neglected. The effects on the model of variations in certain less-defined characteristics of the water tunnel were determined and found to be large, resulting in uncertainty of the model. Because these characteristics are currently unknown, the ideal system model was adopted for use in the current study.

The water tunnel model provides the two required relationships between the dynamic pressure and flow at the inducer inlet and discharge. Both the water tunnel model and the dynamic equations of the cavitating inducer were then modeled on the analog computer to form a closed-loop system for studying the cavitation oscillations. However, although both the inducer and the water tunnel analog models appeared to be stable and yielded correct results in certain individual check tests, the closed-loop system was unstable. These instabilities could probably be eliminated in further studies, permitting comparison of the theory with test data.

STALL OSCILLATIONS

Experience with air compressors has confirmed two types of stall--progressive stall and abrupt stall--each characterized by stall zones which rotate in the pump at speeds of approximately one-half the shaft speed and which generate pressure and flow oscillations in the pump discharge system. Progressive stall is indicated by a smooth continuous loss in pump head at reduced values of flow coefficient, while abrupt stall is characterized by a sharp discontinuous drop in head. The head capacity performance curve of centrifugal pumps generally is characterized by a smooth loss of head indicating a possible progressive stall, and the axial pump has a performance curve characteristic of an abrupt stall.

Both axial and centrifugal pumps were tested in air test facilities to observe experimentally any stall oscillations which might occur. The axial pump was a Mark 26 fuel pump. This pump exhibited an abrupt stall with a characteristic stall hysteresis loop and characteristic stall oscillations with frequencies of approximately one-half the shaft speed and high amplitudes. These data are shown in Fig. 6. The oscillation amplitudes are seen to be four to six times larger during stall.

Three centrifugal pumps were tested, a Mark 10 LOX pump and two Mark 10 fuel pumps with a 6 vane and 6+6 vane impeller. The LOX pump indicated no drop in head, down to almost zero flow. Both fuel pumps had a smooth continuous drop in head, indicating a progressive stall. However, none of the centrifugal pumps evidenced any stall oscillations.

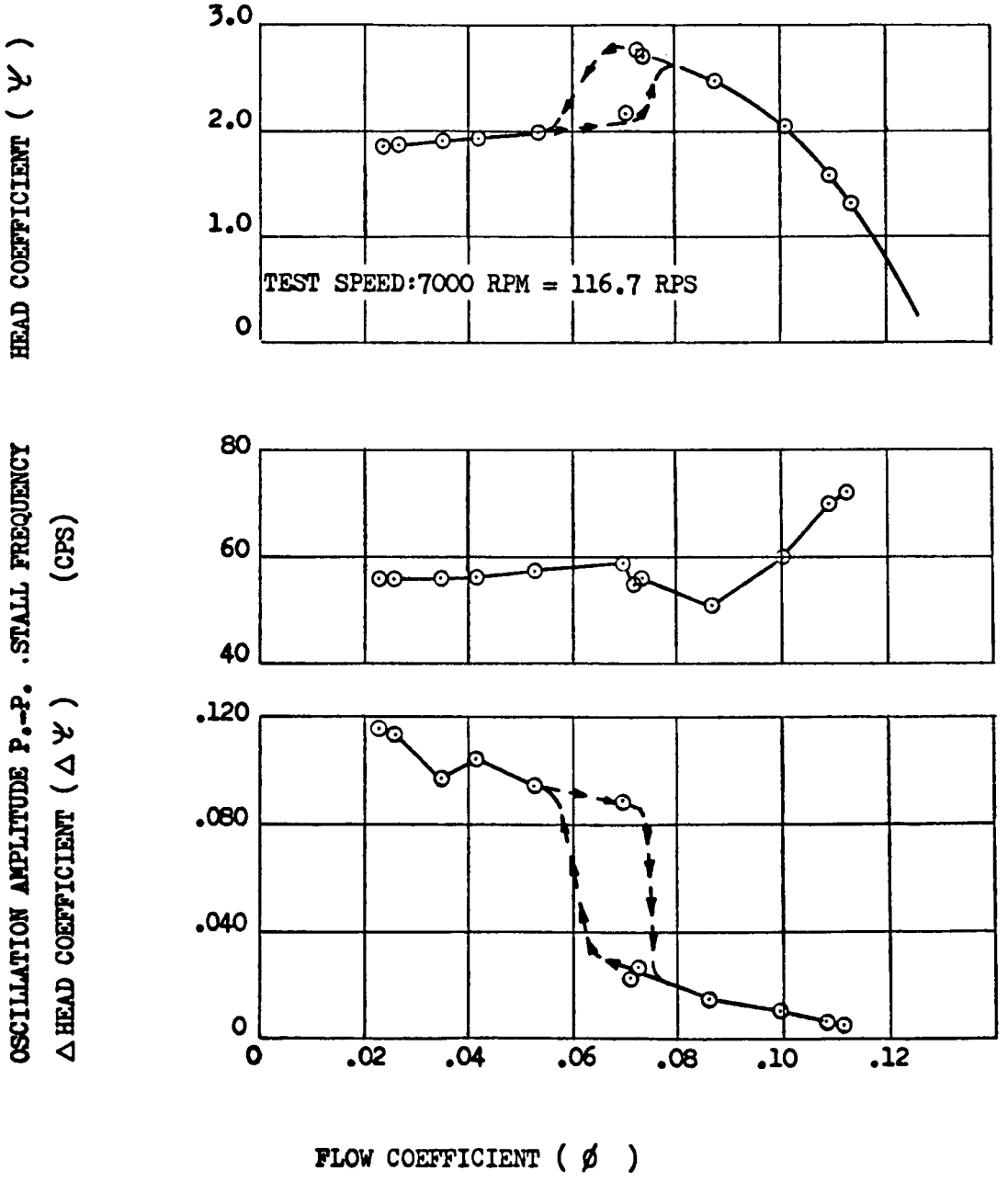

Figure 6. Mark 26 Fuel Pump Stall Oscillation Characteristics

APPENDIX A

NOMENCLATURE

a_{ij}	=	coefficients for curve fit of cavity area
b_i	=	coefficients for curve fit of inducer head rise
c	=	acoustic velocity
D_v	=	mean volute diameter
g	=	acceleration of gravity
G	=	series defining the inertance of a plane discontinuity
j	=	harmonic number or dummy variable
K'	=	constant
ℓ_x	=	width of two-dimensional channel
L	=	inertance
m	=	integer
n,N	=	pump speed in rps and rpm, respectively
N_B	=	number of blades
NPSH	=	net positive suction head
P_1, P_2	=	pressures, e.g., inlet and discharge
P_v	=	vapor pressure
r, r_T, r_H	=	radii, e.g., at tip (T) and hub (H)
R_1, R_2	=	outer and inner radii of curved elbow
s_i	=	tangential distance between the ith diffuser vane and its nearest neighboring impeller vane in the direction opposite to the impeller rotation for a given orientation of impeller and diffuser
S	=	area (with various subscripts)

t	=	time
T_i	=	distance traveled by wave from the discharge of the ith blade to a point of superposition of waves
U_t	=	impeller tip speed
v	=	mean fluid velocity in volute
V_c	=	cavity volume
$\dot{w}_1, \dot{w}_2$	=	weight flowrate
x_c, y_c	=	cavity coordinates
y_m	=	blade thickness coordinate
Y	=	amplitude of superimposed waves divided by amplitude of single wave
Z_d, Z_i	=	number of diffuser and impeller blades, respectively
α	=	angle of incidence
β	=	blade angle
η_i	=	phase angle
λ	=	wavelength of oscillations
ρ	=	fluid density
τ	=	cavitation parameter
φ	=	flow coefficient
ψ_2	=	head rise coefficient
ω	=	circular frequency

REFERENCES

1. Morse, P. M. and K. U. Ingard: "Linear Acoustic Theory," Handbuch Der Physik, Vol. 11, No. 1, 1961.

2. Morse, P. M. and H. Feshbach: Methods of Theoretical Physics. Parts I and II., McGraw Hill Book Co., New York, 1953.

3. Strub, R. A.: "Pressure Fluctuations and Fatigue Stresses in Storage Pumps and Pump-Turbines," A.S.M.E. Trans., Paper No. 63-AHGT-11.

4. Stripling, L. B. and A. J. Acosta: "Cavitation in Turbopumps-Part I," A.S.M.E. Trans., Jour. Basic Engr., September 1962.

APPENDIX B

DISTRIBUTION LIST

	No. of Copies
NASA Marshall Space Flight Center Huntsville, Alabama 35812 Attn: Purchasing Office PR-CH	1
NASA Marshall Space Flight Center Huntsville, Alabama 35812 Attn: Scientific & Technical Information Branch, MS-IP	1
NASA Marshall Space Flight Center Huntsville, Alabama 35812 Attn: Patent Office, CCP	1
NASA Marshall Space Flight Center Huntsville, Alabama 35812 Attn: Technology Utilization Office, MS-T	1
NASA Marshall Space Flight Center Huntsville, Alabama 35812 Attn: Keith Chandler, R-P&VE-PA	1
Chief, Liquid Propulsion Technology, RPL NASA Headquarters, Washington, D. C. 20546	1
Mr. E. Z. Gray Chief, Advanced Manned Missions, MT NASA Headquarters Washington, D. C. 20546	1

	No. of Copies
Mr. Vincent L. Johnson Director, Launch Vehicles and Propulsion, SV Office of Space Science and Applications NASA Headquarters Washington, D. C. 20546	1
Scientific and Technical Information Facility NASA Representative, Code CRT P. O. Box 5700 Bethesda, Maryland, 20014	20
NASA Marshall Space Flight Center Huntsville, Alabama 35812 Attn: Mr. J. Parker, PR-EC, MSFC	5
NASA Marshall Space Flight Center Huntsville, Alabama 35812 Attn: Mr. C. Miller, R-P&VE-PAC, MSFC	6
NASA Marshall Space Flight Center Huntsville, Alabama 35812 Attn: Mr. H. Beduerftig, R-P&VE-P, MSFC	1
NASA Ames Research Center Moffett Field, California 94035 Attn: Technical Librarian for: Harold Hornby Mission Analysis Division	2
NASA Ames Research Center Moffett Field, California 94035 Attn: Technical Librarian for: Clarence A. Syvertson Mission Analysis Division	1
NASA Goddard Space Flight Center Greenbelt, Maryland 20771 Attn: Technical Librarian for: Merland L. Moseson Code 623	2

	No. of Copies
NASA Jet Propulsion Laboratory California Institute of Technology 4800 Oak Grove Drive Pasadena, California 91103 Attn: Technical Librarian for: Henry Burlage, Jr. Prop. Division 38	2
NASA Langley Research Center Langley Station Hampton, Virginia 23365 Attn: Technical Librarian for: Dr. Floyd L. Thompson Director	2
NASA Lewis Research Center 21000 Brookpark Road Cleveland, Ohio 44135 Attn: Technical Librarian for: Dr. Abe Silverstein Director	2
NASA Marshall Space Flight Center Huntsville, Alabama 35812 Attn: Technical Librarian for: Hans G. Paul Code R-P&VE-P	2
NASA Manned Spacecraft Center Houston, Texas 77001 Attn: Technical Librarian for: Robert R. Gilruth Director (Code D)	2
NASA Western Operations Office 150 Pico Boulevard Santa Monica, California 90406 Attn: Technical Librarian for: Robert W. Kamm Director	2

	No. of Copies
NASA John F. Kennedy Space Center Cocoa Beach, Florida 32931 Attn: Technical Librarian for: Dr. Kurt H. Debus	2
Aeronautical Systems Division Air Force Systems Command Wright-Patterson Air Force Base Dayton, Ohio 45433 Attn: Technical Librarian for: Dr. L. Schmidt, Code ASRCNC-2	1
Air Force Missile Development Center Holloman Air Force Base, New Mexico Attn: Technical Librarian for: Major R. E. Bracken, Code MDGRT	1
Air Force Missile Test Center Patrick Air Force Base, Florida Attn: Technical Librarian for: L. J. Ullian	1
Air Force Systems Division Air Force Unit Post Office Los Angeles 45, California Attn: Technical Librarian for: Col. Clark, Tech. Data Center	1
Arnold Engineering Development Center Arnold Air Force Station Tullahoma, Tennessee Attn: Technical Librarian for: Dr. H. K. Doetsch	1
Bureau of Naval Weapons Department of the Navy Washington 25, D. C. Attn: Technical Librarian for: J. Kay, Code RTMS-41	1

	No. of Copies
Defense Documentation Center Headquarters Cameron Station, Building 5 5010 Duke Street Alexandria, Virginia 22314 Attn: TISIA	1
Headquarters, U. S. Air Force Washington, D. C. Attn: Technical Librarian for: Col. C. K. Stambaugh, Code AFRST	1
Picatinny Arsenal Dover, New Jersey 07801 Attn: Technical Librarian for: I. Forsten, Chief Liquid Propulsion Lab	1
Rocket Propulsion Laboratories Edwards Air Force Base Edwards, California 93523 Attn: Technical Librarian for: RPRR/Mr. H. Main	1
U. S. Atomic Energy Commission Technical Information Services Box 62 Oak Ridge, Tennessee Attn: Technical Librarian for: A. P. Huber Oak Ridge Gaseous Diffusion Plant (ORGDP) P.O. Box P	1
U. S. Army Missile Command Redstone Arsenal 35809 Attn: Technical Librarian for: Dr. Walter Wharton	1
U. S. Naval Ordnance Test Station China Lake, California 93557 Attn: Technical Librarian for: Code 4562 Chief, Missile Prop. Div.	1

	No. of Copies
Chemical Propulsion Information Agency Applied Physics Laboratory 8621 Georgia Avenue Silver Spring, Maryland 20910 Attn: Technical Librarian for: Tom Reedy	1
Aerojet-General Corporation P. O. Box 296 Azusa, California Attn: Technical Librarian for: L. F. Kohrs	1
Aerojet-General Corporation P. O. Box 1947 Technical Library, Bldg. 2015, Dept. 2410 Sacramento, California 95809 Attn: Technical Librarian for: R. Stiff	1
Aeronuetronic Philco Corporation Ford Road Newport Beach, California Attn: Technical Librarian for: D. A. Carrison	1
Aerospace Corporation 2400 East El Segundo Boulevard P. O. Box 9508 Los Angeles, California 90045 Attn: Technical Librarian for: John G. Wilder MS-2293 Propulsion Dept.	1
Arthur D. Little, Inc. Acorn Park Cambridge 40, Massachusetts Attn: Technical Librarian for: E. Karl Bastress	1
Astropower, Inc., Subsidiary of Douglas Aircraft Company 2968 Randolph Avenue Costa Mesa, California Attn: Technical Librarian for: Dr. George Moc Director, Research	1

	No. of Copies
Astrosystems International, Inc. 1275 Bloomfield Avenue Caldwell Township, New Jersey Attn: Technical Librarian for: A. Mendenhall	1
Atlantic Research Corporation Edsall Road and Shirley Highway Alexandria, Virginia 22314 Attn: Technical Librarian for: A. Scurlock	1
Beech Aircraft Corporation Boulder Facility Box 631 Boulder, Colorado Attn: Technical Librarian for: J. H. Rodgers	1
Bell Aerosystems Company P. O. Box 1 Buffalo 5, New York Attn: Technical Librarian for: W. M. Smith	1
Bendix Systems Division Bendix Corporation, 3300 Plymouth Road Ann Arbor, Michigan Attn: Technical Librarian for: John M. Brueger	1
Boeing Company P. O. Box 3707 Seattle 24, Washington Attn: Technical Librarian for: J. D. Alexander	1
Chrysler Corporation Missile Division P. O. Box 2628 Warren, Michigan 48231 Attn: Technical Librarian for: John Gates	1

	No. of Copies
Curtiss-Wright Corporation Wright Aeronautical Division Woodridge, New Jersey Attn: Technical Librarian for: G. Kelley	1
Douglas Aircraft Company, Inc. Missile and Space Systems Division 3000 Ocean Park Boulevard Santa Monica, California 90406 Attn: Technical Librarian for: R. W. Hallet Chief Engineer Advanced Space Tech.	1
Fairchild Stratos Corporation Aircraft Missiles Division Hagerstown, Maryland 10 Attn: Technical Librarian for: J. S. Kerr	1
General Dynamics/Astronautics Library & Information Services (128-00) P. O. Box 1128 San Diego, California 92112 Attn: Technical Librarian for: Frank Dore	1
General Electric Company Re-Entry Systems Department 3198 Chestnut St. Philadelphia, Pennsylvania 19101 Attn: Technical Librarian for: F. E. Schultz	1
Advanced Engine & Technology Dept. General Electric Company Cincinnati, Ohio 45215 Attn: Technical Librarian for: D. Suichu	1
Grumman Aircraft Engineering Corp. Bethpage Long Island, New York Attn: Technical Librarian for: Joseph Gavin	1
Kidde Aero-Space Division Walter Kidde and Company, Inc. 675 Main Street Belleville, New Jersey 07109 Attn: Technical Librarian for: R. J. Hanville Director of Research Engineering	1

	No. of Copies
Ling-Temco-Vought Corp. Astronautics P. O. Box 5907 Dallas, Texas 75222 Attn: Technical Librarian for: Warren C. Trent	1
Lockheed California Company 2555 N. Hollywood Way Burbank, California 91503 Attn: Technical Librarian for: G. D. Brewer	1
Lockheed Missiles and Space Company Attn: Technical Information Center P. O. Box 504 Sunnyvale, California Attn: Technical Librarian for: Y. C. Lee	1
Lockheed Propulsion Company P. O. Box 111 Redlands, California Attn: Technical Librarian for: H. L. Thackwell	1
The Marquardt Corporation 16555 Saticoy Street Van Nuys, California 91409 Attn: Technical Librarian for: Warren P. Boardman, Jr.	1
Martin Division Martin Marietta Corporation Baltimore, Maryland 21203 Attn: Technical Librarian for: John Calathes (3214)	1
Denver Division Martin Marietta Corporation P. O. Box 179 Denver, Colorado 80201 Attn: Technical Librarian for: J. D. Goodlette, Mail A-241	1

	No. of Copies
McDonnell Aircraft Corporation P. O. Box 516/Municipal Airport St. Louis, Missouri 63166 Attn: Technical Librarian for: R. A. Herzmark	1
North American Aviation, Inc. Space & Information Systems Division 12214 Lakewood Blvd. Downey, California 90241 Attn: Technical Librarian for: H. Storms	1
Northrop Space Laboratories 3401 West Broadway Hawthorne, California Attn: Technical Librarian for: Dr. William Howard	1
Pratt & Whitney Aircraft Corp. Florida Research and Development Center P. O. Box 2691 West Palm Beach, Florida 33402 Attn: Technical Librarian for: R. J. Coar	1
Radio Corporation of America Astro-Electronics Division Defense Electronic Products Princeton, New Jersey 08540 Attn: Technical Librarian for: S. Fairweather	1
Reaction Motors Division Thiokol Chemical Corporation Denville, New Jersey 07832 Attn: Technical Librarian for: Arthur Sherman	1
Republic Aviation Corporation Farmingdale Long Island, New York Attn: Technical Librarian for: Dr. William O'Donnell	1
Space General Corporation 9200 Flair Avenue El Monte, California 91734 Attn: Technical Librarian for: C. E. Roth	1

	No. of Copies
Space Technology Laboratories Subsidiary of Thompson-Ramo-Wooldridge One Space Park Redondo Beach, California 90278 Attn: Technical Librarian for: G. W. Elverum	1
Stanford Research Institute 333 Ravenswood Avenue Menlo Park, California 94025 Attn: Technical Librarian for: Lionel Dickinson	1
TAPCO Division Thompson-Ramo-Wooldridge, Inc. 23555 Euclid Avenue Cleveland, Ohio 44117 Attn: Technical Librarian for: P. T. Angell	1
Thiokol Chemical Corporation Huntsville Division Huntsville, Alabama Attn: Technical Librarian for: John Goodloe	1
United Aircraft Corporation Research Laboratories 400 Main Street East Hartford, Connecticut 06108 Attn: Technical Librarian for: Erle Martin	1
United Technology Center 587 Methilda Avenue P. O. Box 358 Sunnyvale, California 94088 Attn: Technical Librarian for: B. Abelman	1
Rocket Research Corporation 520 South Portland Street Seattle, Washington 98108 Attn: Technical Librarian for: Foy McCullough, Jr.	1
KAMAN Aircraft Corporation Garden of the Gods Road Colorado Springs, Colorado Attn: Technical Librarian for: K. W. Erickson, V. P. & General Manager	1

	No. of Copies
Worthington Corporation 401 Worthington Avenue Harrison, New Jersey Attn: Technical Librarian for: W. K. Jekat	1
Iowa State University Ames, Iowa Attn: Technical Librarian for: Prof. G. K. Serevy	1
Pennsylvania State College State College, Pennsylvania Attn: Technical Librarian for: Prof. G. Wislicenus	1